Data, Innovation, and Science Cluster

Swarm TII Raw And Corrected Imagery / Spectra (TRACIS) Product Definition

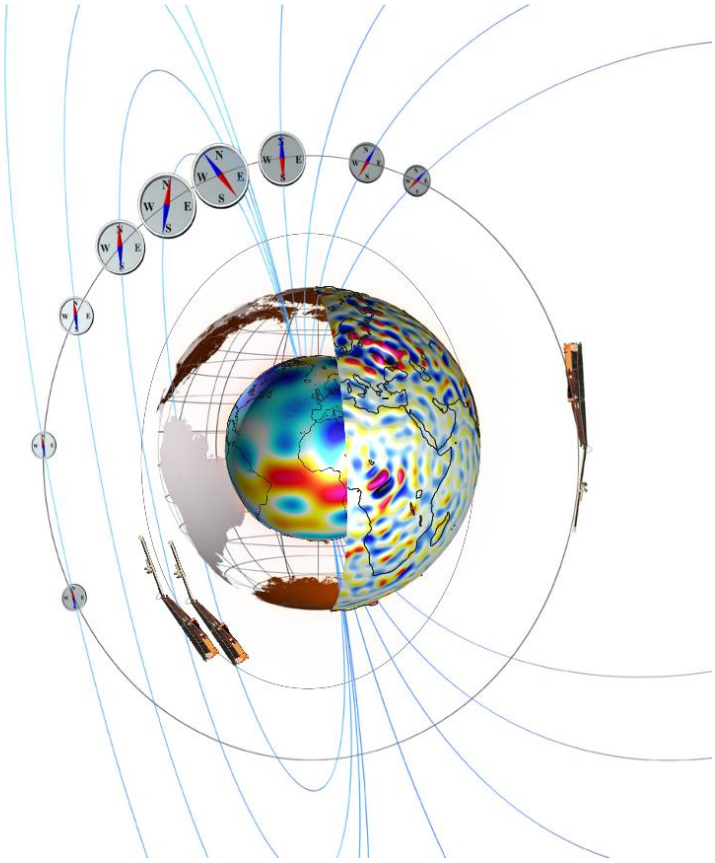

Doc. no: SW-TN-UoC-GS-001: 3, 5 Sep 2023

Johnathan Burchill Date 5 Sep 2023

X

Project Staff

Approved:

David Knudsen Date 5 Sep 2023

Project Manager

Record of Changes

Reason	Description	Rev	Date
Initial vers.	Draft	1dA	17 Aug 2022
Revision	Revised for DTU feedback	1dB	7 Sep 2022
Released	Additional clarifications and corrections requested by DTU. Signed.	1	9 Sep 2022
Revision	Description of version 0102.	2dA	15 Nov 2022
Released	Signed.	2	18 Nov 2022
Revision	Revised algorithm for energy calculation. Description of version 0201.	3dA	11 Apr 2023
Released	Signed.	3	5 Sep 2023

Table of Contents

List of Tables

1 Introduction

This document describes the Swarm TII Raw And Corrected Imagery / Spectra (TRACIS) products.

1.1 Scope and applicability

This document is a deliverable of the Swarm DISC Fast-Track and Space Weather applications task of J100 [AD-1].

2 Applicable and Reference Documentation

2.1 Applicable Documents

The following documents are applicable to the definitions within this document.

[AD-1] SW-OF-UOC-GS-124 DISC contract.

2.2 Reference Documents

The following documents contain supporting and background information relevant to the TRACIS products.

[RD-1] Knudsen, D. J., J. K. Burchill, S. C. Buchert, A. I. Eriksson, R. Gill, J.-E. Wahlund, L. Åhlen, M. Smith, and B. Moffat (2017), Thermal ion imagers and Langmuir probes in the Swarm electric field instruments, J. Geophys. Res. Space Physics, 122, 2655–2673, doi:10.1002/2016JA022571.

[RD-2] SW-IC-CDV-EF-002 Revision U. Swarm EFI Software Interface Design Document.

[RD-3] Burchill, J.K. and Knudsen, D.J., 2022. Swarm Thermal Ion Imager measurement performance. Earth, Planets and Space, 74(1), pp.1-39.

[RD-4] CDF C Reference Manual Version 3.8.1, 10 July 2021, Space Physics Data Facility, NASA / Goddard Space Flight Center

[RD-5] Level 2 Product Format, https://earth.esa.int/eogateway/missions/swarm/product-data-handbook/level-2-product-format, accessed 15 August 2022.

2.3 Abbreviations

A list of acronyms and abbreviations used by Swarm partners can be found here. Any acronyms or abbreviations not found on the online list but used in this document can be found below.

Acronym or abbreviation	***Description***
TRACIS	TII Raw And Corrected Imagery / Spectra

3 Product Description

3.1 Outline

This document provides information about the Swarm TII Raw And Corrected Imagery / Spectra (TRACIS) low and high resolution products. This product represents an official archive of Level 0 TII full images and derived (Level 1b) gain-corrected images and energy and angle-of-arrival count-rate spectra. Data are provided in NASA/CDF files.

The low-resolution (LR) product consists of TII full images and derived products at the variable TII full image cadence, which varies from a few seconds to several minutes according to the operation plan for each satellite. Image quality is characterized with respect to various TII imaging anomalies. The high-resolution (HR) product consists of the Level 0 TII column sum count-rates at a cadence of 2 spectra per second.

Some understanding of the TII principle of operation is required to be able to interpret the ion imagery and spectra. See [RD-1] for details on the imaging technique and [RD-3] for details on theoretical and actual imaging performance (including TII imaging anomalies).

3.2 Methodology

3.2.1 LR product

Raw detector (image) count rates are copied from the Level 0 data. The corrected images have had thresholds subtracted (with negative count rates clamped to 0) and pixel gain corrections applied using the historical gain correction image maps as applied on-board. The gain correction maps have been estimated from flight imagery at various epochs but have not been validated. Energy and angle-of-arrival spectra represent detector count rates rather than physical fluxes. The spectra count rates are normalized to the spectra obtained from a uniform image of signal level 1 DN. Count rates are modulated by variations in MCP voltage and shutter duty cycle (part of an automatic gain control circuit) which affect end-to-end detector gain [RD-1]. These variations have not been factored into the calculation of the ion spectra.

The detector coordinate origin for each sensor has been estimated from flight imagery. The radial coordinate of each pixel is used to estimate the mean kinetic energy of ions detected by that pixel. This includes the gain or loss in ion kinetic energy associated with traversal of the satellite's Debye sheath.

The TII sensor energy maps (transfer functions) are calculated from Monte-Carlo simulations of cold ion beams, for which a third-order polynomial model is estimated from mean radial landing positions and ion energy [RD-3]. Two sets of simulations have been carried out to characterize the sensor energy response for bias grid voltages of -99.0 V and -60.3 V, which are the two predominant operating points for the Swarm TIIs. In cases where the Bias Grid voltages are higher than -60.3 V, the -60.3 V energy transfer function is linearly scaled to the actual bias grid voltage (as happens during TII calibration mode operation, where the bias grid voltage is stepped from -0.8V to -20 V).

The energies at radii smaller than about 5 pixels not included in the energy and angle-of-arrival spectra. Pixels at radii beyond 37 pixels are also not included in the spectra. In the spectra derived from corrected imagery, pixels whose gain correction value is 0 (i.e., cropped pixels) are not included in the spectra. At these locations the energy maps have been set to -1 and the angle-of-arrival maps to -200. There are 20 energy rings spanning radii from 5 pixels to 32 pixels in equal steps. Energy spectra bins represent mean energies over each ring.

Angle-of-arrival refers to detector angles with respect to the CCD coordinate system (rows and columns). Systematic errors in arrival angle associated with manufacturing tolerances are not taken into account. Satellite rotations (yaw and pitch) have not been removed. The arrival angle 0° represents, approximately, the direction of the SCF frame $-x$ axis, i.e., in the direction opposite the satellite motion. Spectra are calculated over 72 sectors spanning -135° and +135°. Angle-of-arrival bins represent mean angles over each sector.

Data are processed in intervals of one day. The image cadence is low in comparison with the 2 Hz TII products, ranging from a couple of seconds in TII calibration mode (one sensor at a time) to every 256 s. Daily science operations have cadences of order 10 s.

Each TII image has a corresponding energy map and angle-of-arrival map. These maps typically do not vary within the course of a (daily) scientific operation. They do vary when the bias grid voltage is modulated, for example when the instrument is operated in TII calibration mode (typically every few months) or during the daily detector scrubbing orbits. A future version of the dataset may incorporate small variations in energy maps associated with changes in MCP voltage.

Image quality flags are calculated as a bit-wise logical OR based on the presence of six different TII imaging anomalies [RD-3]. These flags are described in Section 3.4.1. Incomplete images, arising from missing telemetry for example, are flagged as invalid. In cases where a sensor's image is unavailable (e.g., in TII calibration mode images are sent from only one sensor at a time), the raw and corrected imagery and spectra are filled with zeros.

3.2.2 HR product

Each bin of the 2 Hz column sum product is calculated onboard the EFI from the 8 consecutive full images in each half second after thresholding and gain corrections have been applied. The spectra are copied from the Level 0 source files with no post-processing. In contrast with the LR product energy spectra, normalization is not applied.

Each TII column spans a range of ion energies and angles-of-arrival. Energy bins corresponding to an angle-of-arrival of 0° are provided for each spectrum to aid in their interpretation. The equivalent radius of each bin is converted to energy using the method in Section 3.2.1. In cases where the ion energy is not well defined (typically the first few bins) the bin energy is set to -1 eV and should be disregarded.

3.3 Inputs

TII images are obtained from level 0 files (SW_OPER_EFIXNOM_0_, where X is A, B or C) obtained from PDGS.

Satellite position is obtained from the Swarm MODX_SC_1B data product available from PDGS.

3.4 File format

Daily data of ion temperature estimates are provided in Common Data Format files (CDF) at 2Hz resolution with the following naming convention:

SW_OPER_EFIxTISr1B_YYYYMMDDTHHMMSS_yyyymmddThhmmss_VVVV.cdf

where

- x is the satellite letter, one of A, B or C;
- r is the dataset rate, either L (low rate) or H (high rate);

• YYYYMMDDTHHMMSS marks the beginning of the interval;

• yyyymmddThhmmss marks the end of the interval;

• VVVV is the dataset version.

The CDF files are compressed internally at the variable level.

3.4.1 TISL1B product file format

Table 1. TRACIS TISL1B product definition

Product Identifier	SW_OPER_EFIxTISL1B
Definition	Raw and corrected TII imagery, ion energy and angle count rate spectra, and TII imaging anomaly flags.
Input Data	SW_OPER_EFIxNOM_0_ (Level 0 EFI data) SW_OPER_MODA_SC_1B (Level 1B ephemeris data)
Input Time Span	1 day
Spatial representation	Measurements along the Swarm satellite's orbit.
Time representation	Images correspond to 50 ms integration period, obtained at intervals of 1 s to 256 s when the EFI is operating.
Units	Various
Resolution	N/A
Uncertainty	N/A
Quality Indicator	Bitwise-OR'd flags
Data Volume	Variable (daily file with GZIP compression per variable). Typical size 18 MB
Data Format	CDF
Output Data	CDF file with time series (refer to Table 2)
Output Time Span	1 day
Update Rate	Daily
Latency	4 days

Table 2. TRACIS TISL1B CDF fields

Variable	CDF Type	Unit	Note
Timestamp	CDF_EPOCH		UTC
Latitude	CDF_REAL8	deg	Geocentric latitude of orbit
Longitude	CDF_REAL8	deg	Geocentric longitude of orbit
Radius	CDF_REAL8	m	Geocentric radius of orbit
Raw_image_H	CDF_UINT2	DN	40x66 array of raw image data for TII H sensor
Raw_image_V	CDF_UINT2	DN	40x66 array of raw image data for TII V sensor
Processed_image_H	CDF_UINT2	DN	40x66 array of gain-corrected image data for TII H sensor
Processed_image_V	CDF_UINT2	DN	40x66 array of gain-corrected image data for TII V sensor
Valid_imagery_H	CDF_UINT1		0: no or partial image; 1: full image (H sensor)
Valid_imagery_V	CDF_UINT1		0: no or partial image; 1: full image (V sensor)
TII_imaging_mode	CDF_UINT1		Imaging mode. 0: non-nominal; 1: nominal science
Image_anomaly_flags_H	CDF_UINT1		H sensor bit-wise OR'd imaging anomaly flags.
Image_anomaly_flags_V	CDF_UINT1		V sensor bit-wise OR'd imaging anomaly flags.
CCD_dark_current_H	CDF_UINT2	DN	H sensor CCD dark current (from a single pixel)
CCD_dark_current_V	CDF_UINT2	DN	V sensor CCD dark current (from a single pixel)
CCD_temperature_H	CDF_REAL4	deg. C	H sensor CCD temperature (derived from dark current)
CCD_temperature_V	CDF_REAL4	deg. C	V sensor CCD temperature (derived from dark current)
V_MCP_H	CDF_REAL4	V	H sensor MCP front voltage
V_MCP_V	CDF_REAL4	V	V sensor MCP front voltage
V_Phos_H	CDF_REAL4	V	H sensor phosphor voltage

Variable	CDF Type	Unit	Note
V_Phos_V	CDF_REAL4	V	V sensor phosphor voltage
V_Bias_H	CDF_REAL4	V	H sensor inner dome bias voltage
V_Bias_V	CDF_REAL4	V	V sensor inner dome bias voltage
V_Faceplate	CDF_REAL4	V	Faceplate voltage
Shutter_duty_cycle_H	CDF_REAL4		H sensor electrostatic shutter open duty cycle
Shutter_duty_cycle_V	CDF_REAL4		V sensor electrostatic shutter open duty cycle
Energy_map_H	CDF_REAL4	eV	H sensor pixel kinetic energy map
Energy_map_V	CDF_REAL4	eV	V sensor pixel kinetic energy map
Angle_of_arrival_map_H	CDF_REAL4	eV	H sensor pixel angle-of-arrival map
Angle_of_arrival_map_V	CDF_REAL4	eV	V sensor pixel angle-of-arrival map
Energy_spectrum_H	CDF_REAL4		H sensor ion kinetic energy spectrum (adjusted detector counts)
Energy_spectrum_V	CDF_REAL4		V sensor ion kinetic energy spectrum (adjusted detector counts)
Angle_of_arrival_spectrum_H	CDF_REAL4		H sensor ion angle-of-arrival spectrum (adjusted detector counts)
Angle_of_arrival_spectrum_V	CDF_REAL4		V sensor ion angle-of-arrival spectrum (detector counts)
Raw_energy_spectrum_H	CDF_REAL4		H sensor ion kinetic energy spectrum from uncorrected image (detector counts)
Raw_energy_spectrum_V	CDF_REAL4		V sensor ion kinetic energy spectrum from uncorrected image (detector counts)
Raw_angle_of_arrival_spectrum_H	CDF_REAL4		H sensor ion angle-of-arrival spectrum from uncorrected image (detector counts)
Raw_angle_of_arrival _spectrum_V	CDF_REAL4		V sensor ion angle-of-arrival spectrum from uncorrected image (detector counts)
Energies_H	CDF_REAL4	eV	H sensor energy spectrum energies

Variable	CDF Type	Unit	Note
Energies_V	CDF_REAL4	eV	V sensor energy spectrum energies
Angles_of_arrival	CDF_REAL4	°	Angle-of-arrival spectrum angles (both sensors)

Burchill and Knudsen (2022) describe the TII imaging anomalies. The TRACIS TISL1B product imaging anomaly flags are calculated from the bitwise OR of the anomaly values in Table 3 for each anomaly detected. Separate flags are provided for the H and V sensors.

Table 3. TII image anomaly flags

Flag value	Description
0	No anomalies detected.
1	Classic wing anomaly detected.
2	Upper Angel's wing anomaly detected.
4	Lower Angel's wing anomaly detected.
8	Peripheral anomaly detected.
16	Measles anomaly detected.
32	Bifurcation anomaly detected.

3.4.2 TISH1B product file format

Table 4 TRACIS TISH1B product definition

Product Identifier	SW_OPER_EFIxTISH1B
Definition	2 Hz TII column sum spectra as a function of ion energy.
Input Data	SW_OPER_EFIxNOM_0_ (Level 0 EFI data) SW_OPER_MODA_SC_1B_ (Level 1B ephemeris data)
Input Time Span	1 day
Spatial representation	Measurements along the Swarm satellite's orbit.
Time representation	Column sum spectra obtained a cadence of 0.5 s when the EFI is operating.
Units	Various

Resolution	N/A
Uncertainty	N/A
Quality Indicator	N/A
Data Volume	Variable (daily file with GZIP compression per variable). Typical size 7 MB
Data Format	CDF
Output Data	CDF file with time series (refer to Table 5)
Output Time Span	1 day
Update Rate	Daily
Latency	4 days

Table 5. TRACIS TISH1B CDF fields

Variable	CDF Type	Unit	Note
Timestamp	CDF_EPOCH		UTC
Latitude	CDF_REAL8	deg	Geocentric latitude of orbit
Longitude	CDF_REAL8	deg	Geocentric longitude of orbit
Radius	CDF_REAL8	m	Geocentric radius of orbit
TII_imaging_mode	CDF_UINT1		Imaging mode. 0: non-nominal; 1: nominal science
V_MCP_Setting_H	CDF_REAL4	V	H sensor MCP front voltage setting
V_MCP_ Setting_V	CDF_REAL4	V	V sensor MCP front voltage setting
V_Phos_ Setting_H	CDF_REAL4	V	H sensor phosphor voltage setting
V_Phos_ Setting_V	CDF_REAL4	V	V sensor phosphor voltage setting
V_Bias_ Setting_H	CDF_REAL4	V	H sensor inner dome bias voltage setting
V_Bias_ Setting_V	CDF_REAL4	V	V sensor inner dome bias voltage setting
Column_sum_spec-trum_H	CDF_UINT2	DN	H sensor column sum spectrum

Variable	CDF Type	Unit	Note
Column_sum_spectrum_V	CDF_UINT2	DN	V sensor column sum spectrum
Column_sum_energies_H	CDF_REAL4	eV	H sensor column sum spectrum energies
Column_sum_energies_V	CDF_REAL4	eV	V sensor column sum spectrum energies

3.5 Validation and Known Issues

The TRACIS dataset generator software has undergone validation for a limited set of examples primarily through inspection of the product by an expert. Level 0 voltage monitor values have been calculated using conversions reported in [RD-2]. The resulting voltages do not include temperature corrections and have not been validated. CCD temperatures are estimated from dark pixel signal using a nominal transfer function and have not been validated.

Stationary systematic errors in the TII sensor detector origins resulting from manufacturing tolerances in the alignment of the analyzer optics may be present, giving rise to systematic errors in the ion spectra energies and angles-of-arrival.

Gain correction maps have not been validated. In consequence, image count rates should be assumed to have significant uncertainty, perhaps at times exceeding 20% within a given image. Some features of the images and spectra result from TII imaging anomalies ([RD-1] and [RD-3]) and so users should exercise care in interpreting the data.

The TII Monte Carlo simulator, which was used to determine the TII sensor energy maps (transfer functions) has been validated to some extent through simulation of laboratory ion beams. The simulations relevant to operation in orbit assume a thin-sheath approximation for the Debye sheath associated with spacecraft charging. Systematic errors are present in the transfer functions to the extent that this approximation does not capture the actual (and time-varying) sheath. Variations in MCP voltage affect the energy transfer functions; these are taken into account in the estimation of energy spectra using a model for energy parameterized by first-order polynomial in MCP voltage and third-order polynomial in detector radius. The model parameters are determined from least-squares fitting first moments calculated from a series of TII Monte-Carlo simulator images.

4 Releases

4.1 OPER 0101

First release. This version covers the period 9 December 2013 through 4 August 2022.

The effect of MCP voltage on the energy transfer functions, expected to be small, is not modelled. The effect may be incorporated into a later TRACIS version.

4.2 OPER 0102

This version corrects a timing error in the ephemeris that affected geographic position (by about one degree of latitude).

4.3 OPER 0201

This version implements refinements to the energy spectra taking the measured MCP voltage for each sensor into account.